Heliyon 9 (2023) e19907

Contents lists available at ScienceDirect

Heliyon

journal homepage: www.cell.com/heliyon

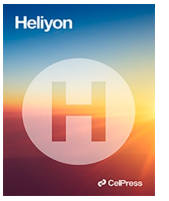

The construction and validation of ECM-related prognosis model in laryngeal squamous cell carcinoma

Xue-fan Jiang, Wen-jing Jiang *

Department of Otolaryngology, Center of Otolaryngology-head and Neck Surgery, Zhejiang Provincial People's Hospital, People's Hospital of Hangzhou Medical College, Hangzhou, 310014, Zhejiang, China

ARTICLE INFO

Keywords:
Extracellular matrix
Laryngeal squamous cell carcinoma
Disease free survival
Risk model
Prediction

ABSTRACT

Background: Laryngeal squamous cell carcinoma (LSCC) is a kind of common and aggressive tumor with high mortality. The application of molecular biomarkers is useful for the early diagnosis and treatment of LSCC.

Methods: The expression and clinical information were obtained from The Cancer Genome Atlas (TCGA) database. Principal components analysis (PCA) was used to discriminate between LSCC and normal samples. The hub genes were screened out through univariate and multivariate cox analyses. The Kaplan-Meier (K-M) and receiver operating characteristic (ROC) curve was used to validate the predictive performance. The single sample gene set enrichment analysis (ssGSEA), Gene Ontology (GO) and Kyoto Encyclopedia of Genes and Genomes (KEGG) analysis were used to determine the enrichment function. Protein-Protein Interaction (PPI) network was constructed in STRING. The immune analysis was performed by ESTIMATE, IPS and xCELL. The drug sensitivity was identified with GSCA database.

Results: We identified that 47 extracellular matrix (ECM) genes were differentially expressed in LSCC compared with normal group. Univariate and multivariate cox analysis determined that leucine-rich glioma-inactivated 4 (LGI4), matrilin 4 (MATN4), microfibrillar-associated protein 2 (MFAP2) and fibrinogen like 2 (FGL2) were closely related to the disease free survival (DSS) of LSCC. ROC curve determined that the risk model has a good predictive performance. PPI network showed the top 100 genes with high correlation of hub genes. The ssGSEA, GO and KEGG enrichment analyses determined that immune response was significantly involved in the development of LSCC. Immune infiltration analysis showed that most immune cells and immune checkpoints were inhibited in high risk score group. Drug sensitivity analysis showed that MATN4, FGL2 and LGI4 were negatively related to various drugs, while MFAP2 was positively related to many drugs.

Conclusion: We established a risk model constructed with four ECM-related genes, which could effectively predict the prognosis of LSCC.

1. Introduction

Head and neck squamous cell carcinoma (HNSC) is a common malignant tumor all over the world, and it has a high incidence

* Corresponding author. Department of Otolaryngology, Center of Otolaryngology-head and neck surgery, Zhejiang Provincial People's Hospital, People's Hospital of Hangzhou Medical College, No.158 Shangtang Road, Gongshu District, Hangzhou, 310014, Zhejiang, China.
E-mail address: jiangwen202302@163.com (W.-j. Jiang).

https://doi.org/10.1016/j.heliyon.2023.e19907
Received 16 February 2023; Received in revised form 23 August 2023; Accepted 5 September 2023
Available online 6 September 2023

among all cancers ranked sixth [1]. Laryngeal squamous cell carcinoma (LSCC) is a common and aggressive tumor of HNSC and derives from the laryngeal mucosal epithelium, which has high mortality [2–4]. At present, the treatments extensively applied to LSCC include surgical resection, chemotherapy and radiotherapy [5]. Although these methods could be controlled with high probability, patients with LSCC are usually diagnosed in an advanced stage [6,7]. Meanwhile, immunotherapy is becoming a promising treatment for numerous cancers including LSCC [8]. Thus, identifying novel biomarkers is vital for the diagnosis and treatment of LSCC.

Extracellular matrix (ECM) consists of fibrillar and structural proteins, proteoglycans, integrins and proteases, and it is a noncellular component of the tumor microenvironment (TME) [9]. Besides, ECM plays a key role in maintaining organizational structure and function [10]. Moreover, more and more studies claimed that ECM was involved in the development of tumors [11]. On the one hand, the abundance changes of ECM components frequently result in the alteration of tissue density and stiffness, which affects the migration of tumor cells through regulating mechanosensing and angiogenesis [12,13]. On the other hand, ECM is a repository for growth factors and cytokines which could promote the development of tumor cells, and the degradation of ECM may cause the release of growth factors and cytokines [14]. It indicates that the degradation of ECM generally accompanies the growth and development of tumors [15,16]. Additionally, ECM is also involved in the regulation of signal pathways through interactions between numerous components and receptors [17,18]. It has been proven that the signal pathways induced by ECM stiffening are related to the growth and metastasis of tumors through activation of angiogenesis, promotion of immune evasion and alteration of drug resistance [19]. As the function of ECM was identified in drug sensitivity, ECM related genes could be a valuable target for clinical treatment [20]. Recently, Zhang et al. identified that the downregulated expression of matrix metallopeptidase 1 (MMP1), a core gene of ECM, led to the inhibition of cell proliferation and migration in HNSCC, especially in hypopharyngeal cancer (35426219). Moreover, some previous studies claimed that the ECM-related risk model could effectively predict the prognosis in non-small cell lung carcinoma and bladder cancer (36404344, 35450397). However, there were few studies about the biological significance of ECM genes in LSCC, and the predictive value of ECM in LSCC was not reported.

Thus, in this study, we first tried to establish a prognosis model based on ECM-core genes. After we determined the prognosis value of this model, we explored the potential internal correlation of risk score in the aspect of signal pathways, immune response. Furthermore, we further analyzed the drug sensitivity of hub genes, which could improve the theoretical basis for the treatment of LSCC.

2. Methods

2.1. Data collection

The mRNA expression profile and corresponding clinical information of LSCC were collected from The Cancer Genome Atlas (TCGA, https://portal.gdc.cancer.gov) and GEO (https://www.ncbi.nlm.nih.gov/geo/) databases. Besides, ECM genes were determined in Matrisome Project (http://matrisomeproject.mit.edu/ecm-atlas/), and 239 ECM core genes were used for the further experiments. The genes differentially expressed in different groups were determined by R package limma (version 3.40.6).

2.2. Principal components analysis (PCA)

The R software package stats (version 4.2.2) was used for the analysis of PCA. In detail, we first carried out z-score on the expression profile, and then the prcomp function was used for dimensionality reduction analysis to obtain the dimensionality reduced matrix.

2.3. The identification of differentially expressed genes (DEGs)

To identify the differentially expressed ECM core genes in LSCC in comparison with the normal group, the t. test function was performed with the R software, and the intersection of these genes in TCGA and GEO datasets was screened out.

2.4. The construction and validation of the risk model

At first, the hub genes were determined by univariate and multivariate cox analysis in SPSS 25. The univariate cox analysis was performed to identify the prognosis genes with $p < 0.05$. Then, these genes were further screened out through multivariate cox analysis with $p < 0.05$ Next, we constructed the risk model based on the regression coefficient of multivariate cox analysis. Then, we calculated the risk score according to the gene expression and corresponding regression coefficient. Furthermore, R package pROC (version 1.17.0.1) was used to calculate the area under the curve (AUC), and the roc function of pROC was used to validate the predictive efficiency of the risk model at 1-, 3- and 5-year survival.

2.5. Survival analysis

The Kaplan–Meier (K-M) curve with hazard ratio (HR) and 95% confidence interval (CI) was used to evaluate the prognosis between two risk groups. Firstly, we calculated the optimal truncation value of risk score using the maxstat of the R package, and the cases of LSCC were divided into two groups according to the value. Then we assessed the difference between the two groups in the prognosis using the survfit function of the R package.

2.6. Single sample gene set enrichment analysis (ssGSEA)

The c2. cp.kegg.v7.4. symbols.gmt subset was obtained from the Molecular Signatures database. The expression and phenotype were integrated and loaded in R software. The R package GSVA was applied to calculate the enrichment score of every sample.

2.7. Protein-protein interaction (PPI) network

The PPI network of hub genes was established in STRING. The cut-off value of the interaction score was 0.4. Besides, the number of 1st shell and 2nd shell was no more than 50 interactors.

2.8. Gene Ontology (GO) and Kyoto Encyclopedia of Genes and Genomes (KEGG) enrichment analysis

The related genes determined by the PPI network were used for the enrichment analysis. The gene set c2. cp.kegg.v7.4. symbols and c5. go.v7.4. symbols were respectively used for the KEGG and GO analysis using the R package clusterProfiler (version 3.14.3). The minimum gene was set to 5 and the maximum gene was set to 5000. The p-value<0.05 was considered statistically significant. The results were visualized by R package GOplot.

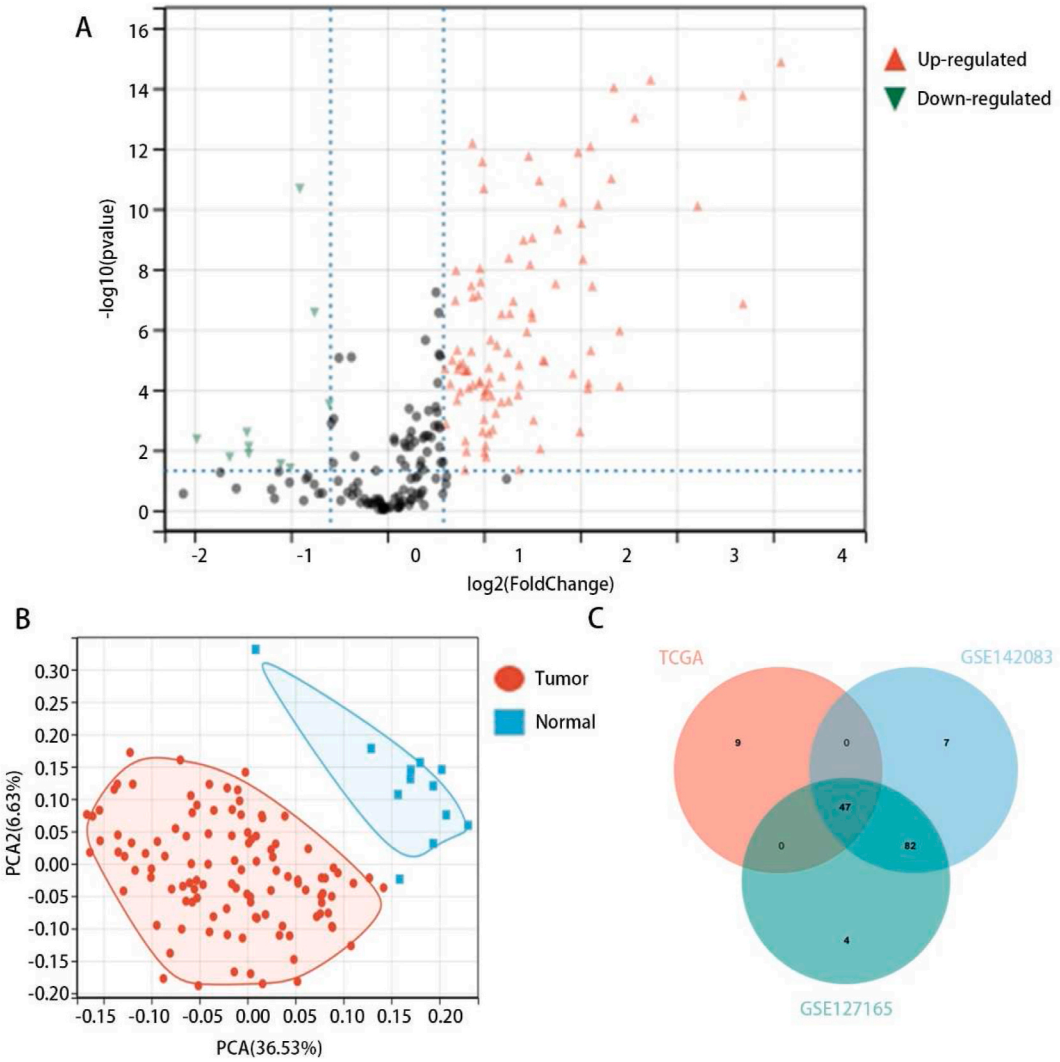

Fig. 1. The identification of the ECM core gene. (A) The expression of ECM core genes in LSCC compared with normal. (B) The normal and tumor samples were distinguished by PCA according to ECM core genes. (C) Venn diagram of differentially expressed ECM core genes in the TCGA, GSE127165 and GSE142083 datasets.

2.9. Immune analysis

The R package IOBR was performed to calculate the immune enrichment score. The algorithm of ESTIMATE was used to calculate the immune and stromal scores of every sample. IPS was performed to assess the enrichment scores after the immune genes were divided into four types, namely effector cells (EC), suppressor cells (SC), major histocompatibility complex (MHC) molecules, and checkpoint (CP). Additionally, the xCELL algorithm was applied to evaluate the enrichment score of every sample in 64 cells.

2.10. Drug sensitivity

Gene Set Cancer Analysis (GSCA) is an integrated platform for the analysis of gene expression, immune response, mutation and drug sensitivity. We assessed the relationship between gene expressions and drug sensitivity in GSCA according to the Genomics of Drug Sensitivity in Cancer (GDSC) and The Cancer Therapeutics Response Portal (CTRP) database.

2.11. Statistics

In this study, all data were analyzed in SPSS 25. The independent sample *t*-test was used to calculate the difference between the two groups, while one-way analysis of variance (ANOVA) was used to determine the difference among multiple groups followed by post-hoc comparisons. The survival difference between the 2 groups was evaluated by the log-rank test, and the correlation analysis was identified by the Pearson test. $p < 0.05$ was considered a significant difference.

3. Results

3.1. The identification of DEGs related to ECM

As shown in Fig. 1A, the expression levels of 39 ECM core genes were notably increased, while 17 genes expression were notably decreased in LSCC compared with normal tissues according to the TCGA dataset. Additionally, the results of PCA showed that the ECM core genes could differentiate LSCC from normal tissues, which suggested that ECM core genes play a vital role in the development of LSCC. Besides, the ECM core genes differentially expressed in GSE127165 and GSE142083 were determined by limma with $p < 0.05$. Then, 47 common ECM core gene set was derived with the use of Venn diagram based on the intersection of TCGA, GSE127165 and GSE142083.

3.2. The identification of hub genes

In addition, univariate cox analysis on 47 genes identified that 16 genes were closely related to disease free survival (DSS) in LSCC ($p < 0.05$). Then, multivariate cox analysis was performed to further determine the prognosis genes. The result demonstrated that four hub genes, namely leucine-rich glioma-inactivated 4 (LGI4), matrilin 4 (MATN4), microfibrillar-associated protein 2 (MFAP2) and fibrinogen like 2 (FGL2), could be closely associated with the DSS of LSCC ($p < 0.05$) (Table 1). Therefore, a four-signature risk model was constructed. Risk score = $(-0.53 \times \text{LGI4}) + (-0.62 \times \text{MATN4}) + 0.678 \times \text{MFAP2} + (-0.31 \times \text{FGL2})$. Furthermore, samples were grouped into high and low risk group according to the optimal truncation value, and we explored the prognosis value of risk score through survival analysis. The K-M results showed that low risk score group had a better prognosis compared with high risk score group (Fig. 2A). Additionally, the receiver operating characteristic (ROC) curve was applied to evaluate the accuracy of risk model. As presented in Fig. 2B, the AUC of 1-, 3- and 5-year survival was respectively 0.77, 0.88 and 0.85, which suggested that the four signatures model could steadily and effectively predict the DSS time of LSCC. From Fig. 2C, it was obvious that the survival time of patients decreased following the increase in risk score.

3.3. The association between risk score and clinical characteristics in LSCC

Next, we analyzed the effect of clinical characteristics on the risk score (Fig. 3A–G). Because the number of patients diagnosed with T1 stage and pathological stage I was too few, we combined patients from T1 and T2 or stage I and II group into one group. From Fig. 3A–D, F-G, there was no significant difference of risk score among different age, gender, M stage, T stage, pathological stage and

Table 1
The univariate and multivariate cox analysis of ECM core genes.

Variables	Univariate cox analysis				Multivariate cox analysis			
		95% of HR				95% of HR		
	HR	lower	upper	*p*-value	HR	lower	upper	*p*-value
LGI4	0.53	0.36	0.78	0.01	0.61	0.41	0.90	0.001
MATN4	0.60	0.40	0.90	0.001	0.54	0.37	0.79	0.02
MFAP2	1.52	1.07	2.16	0.001	1.97	1.32	2.94	0.02
FGL2	0.73	0.55	0.97	0.04	0.70	0.50	0.98	0.03

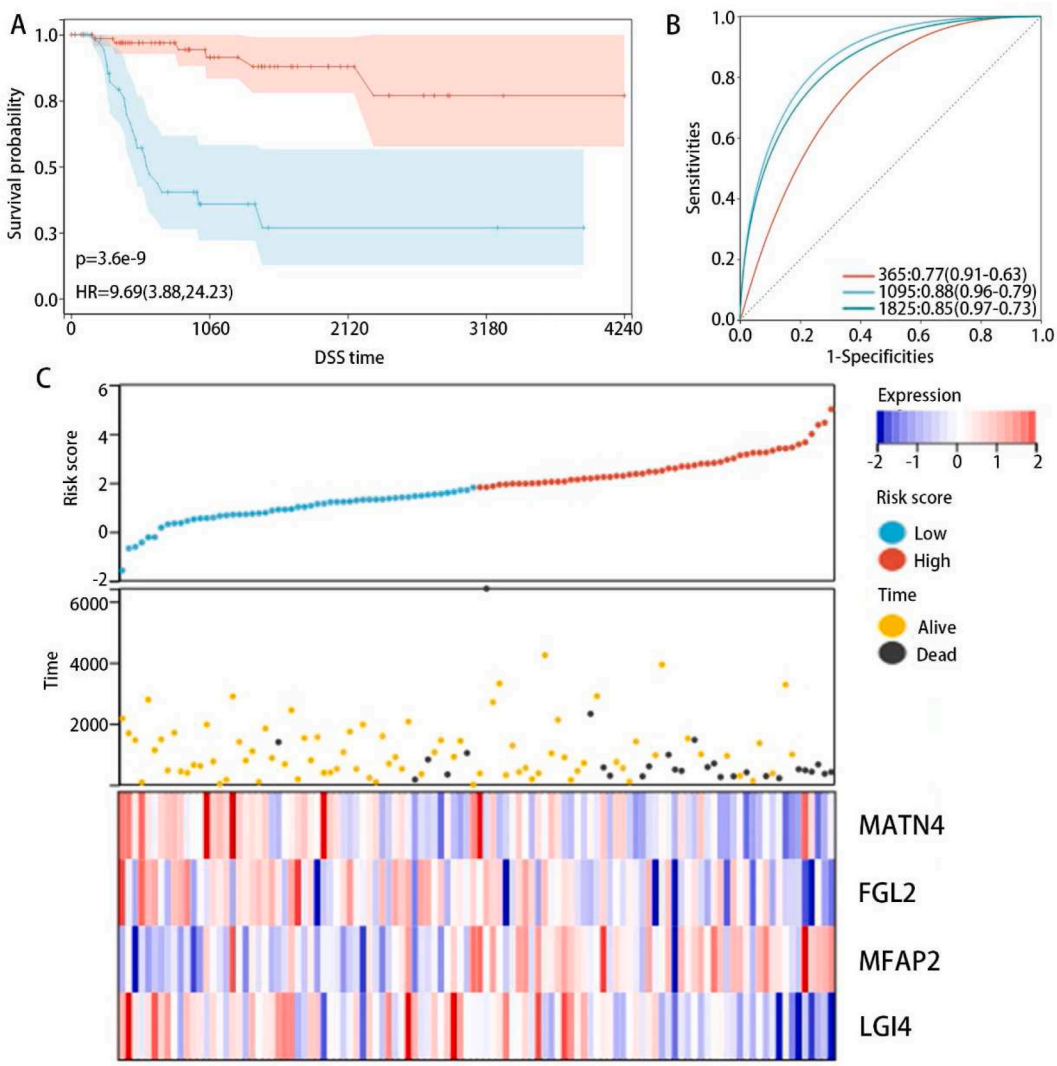

Fig. 2. The construction and identification of risk model. (A) The survival curve between risk score and DSS time in LSCC. (B) The time-dependent ROC analysis of risk score and DSS time in LSCC. (C) The distribution of risk score, survival time, survival status and four signatures in DSS time in LSCC.

smoking history. However, the risk score was obviously affected by N stage, and the patients diagnosed with N3 stage had the highest risk score (Fig. 3E).

3.4. The interaction of risk score with signal pathways

To explore the potential mechanism of signatures in LSCC development, the ssGSEA was executed. As shown in Fig. 4, it was clear that risk score was negatively and remarkably correlated with many signal pathways, including the T cell receptor signaling pathway, B cell receptor signaling pathway, toll like receptor signaling pathway and natural killer cell mediated cytotoxicity, which were involved in the immune process. It suggested that signatures may be closely correlated with immunoreaction.

3.5. The construction of the PPI network and function analysis of DEGs

Besides, to explore the mechanism of four signatures in the aspect of protein, we first constructed a PPI network, and the top 100 genes with the highest interaction score were screened out (Fig. 5). According to the mRNA expression profile, differentially expressed genes were screened out and used for the enrichment analysis. The GO enrichment analysis showed that these genes were involved in cell adhesion, immune system process, response to stress, immune response and cell differentiation in terms of biological process (BP) (Fig. 6A). In the aspect of cellular component (CC), the results displayed that DEGs were enriched in the extracellular region, cell

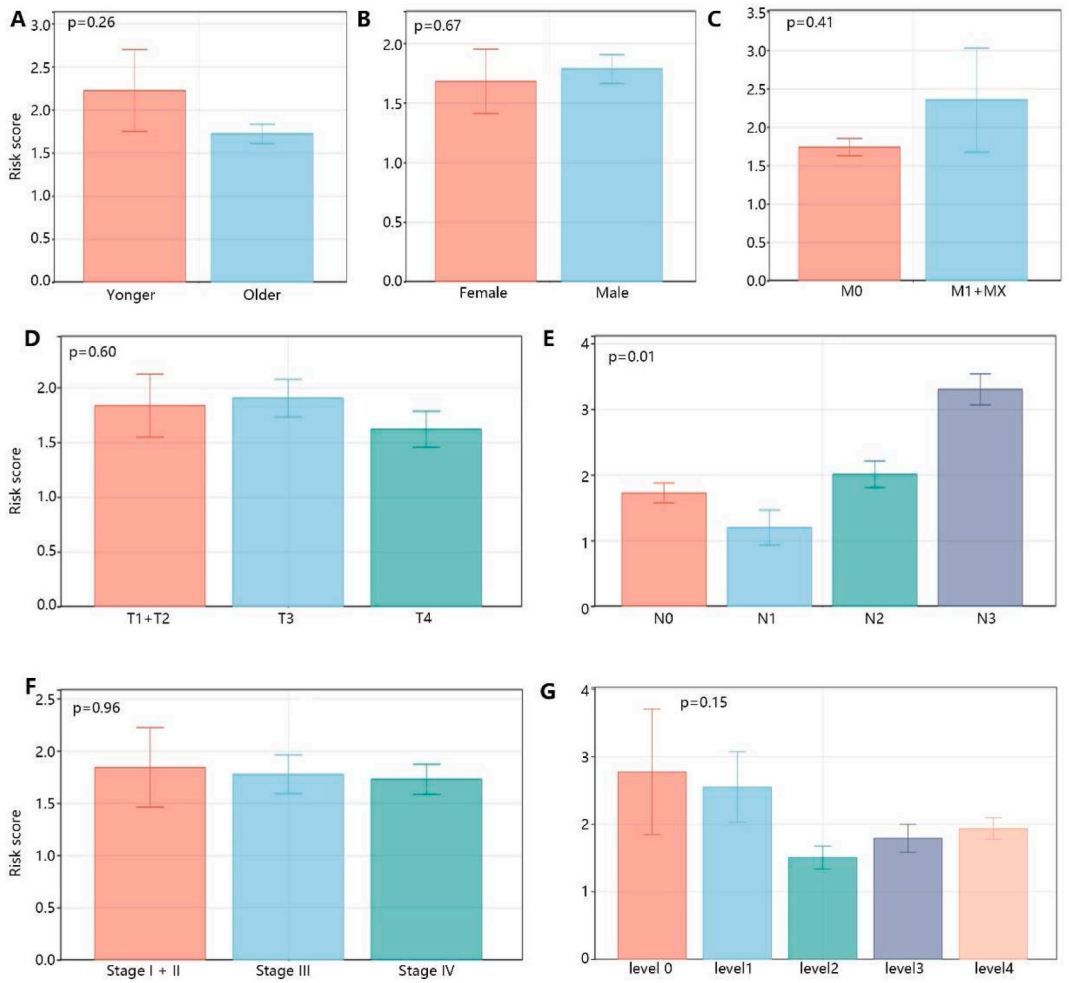

Fig. 3. The risk score in LSCC with different clinical subgroups. (A) age, (B) gender, (C) M stage, (D) T stage, (E) N stage, (F) pathological stage, (G) smoking history.

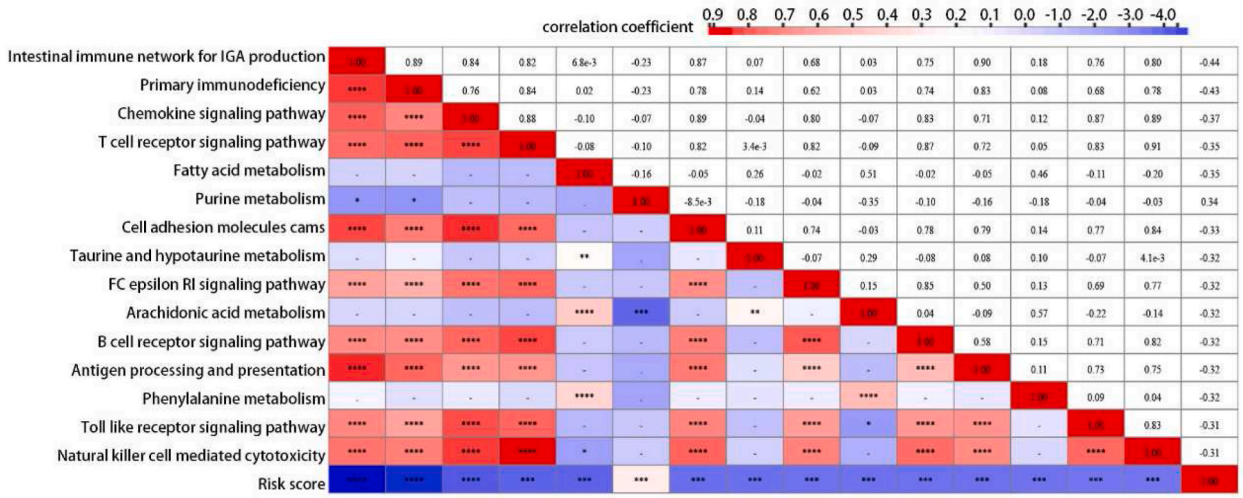

Fig. 4. The relationship between signal pathways and risk scores based on ssGSEA. *<0.05, **<0.01, ***<0.001, ****<0.0001.

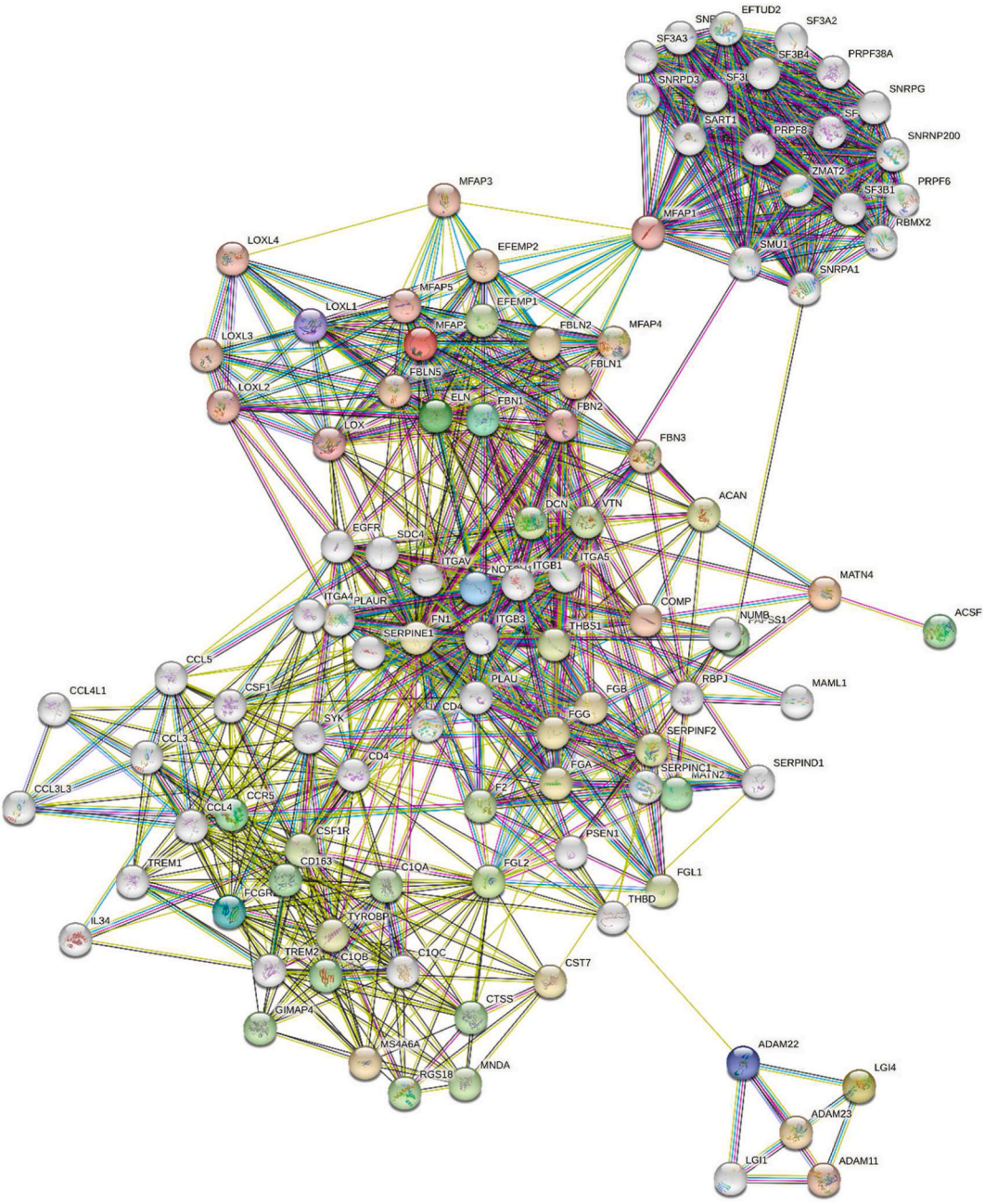

Fig. 5. The PPI network was established based on four signatures.

surface, extracellular space, protein-containing complex and vesicle (Fig. 6B). Additionally, cell adhesion, molecule binding, signaling receptor binding, protein-containing complex binding and signaling receptor activity RNA binding were enriched in molecular function (MF) analysis (Fig. 6C). The KEGG enriched signal pathway contained ECM-receptor interaction, focal adhesion, Phosphatidylinositol-4,5-bisphosphate 3-kinase (PI3K)- protein kinase B (AKT) signaling pathway, notch signaling pathway and toll-like receptor (Fig. 6D), and some of them were involved in the immune process.

3.6. The immune landscape of risk score

To confirm the function of the risk score in the immune process, immune infiltration analysis was performed. From Fig. 7A, it was obvious that the immune score and ESTIMATE score were significantly higher in high risk score group than low risk score group. Furthermore, IPS analysis exhibited that MHC and EC level were significantly upgraded, while SC and CP level were significantly

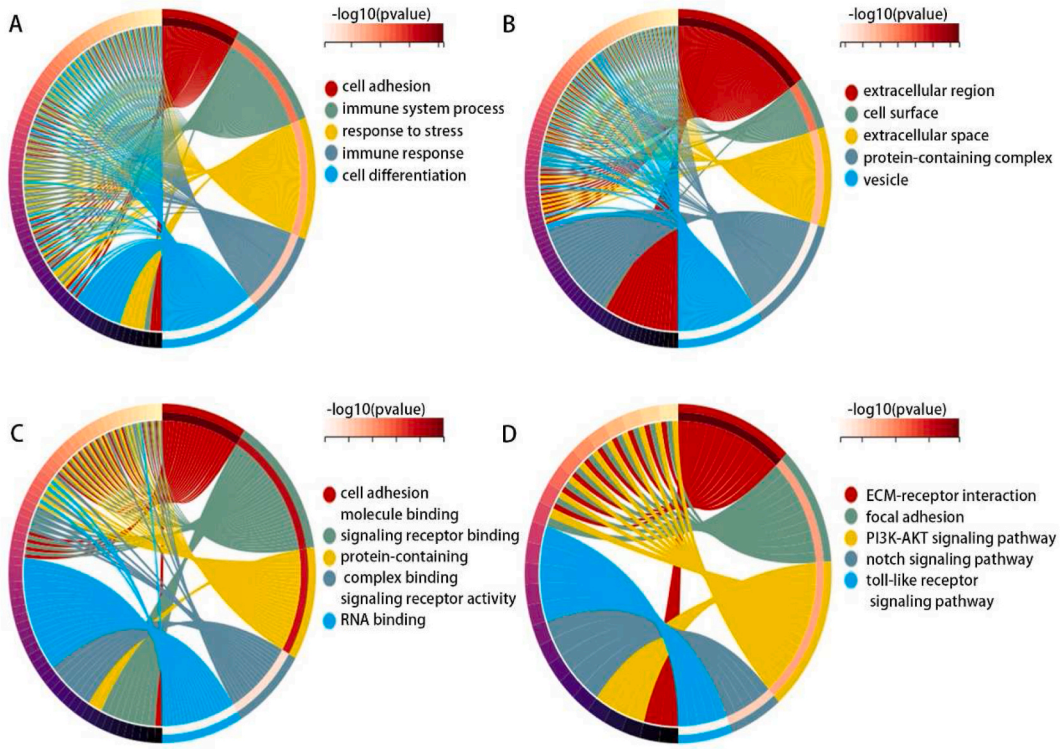

Fig. 6. The GO and KEGG analysis of DEGs in LSCC. (A) The BP of GO analysis, (B) The CC of GO analysis, (C) The MF of GO analysis, (D) KEGG term.

downgraded (Fig. 7B). Next, the xCELL were used to determine the relationship between risk score and various immune cells. The results revealed that risk scores were significantly and positively correlated to 23 immune cells but negatively related to smooth muscle (Fig. 7C). Besides, From Fig. 7D, it can be observed that the levels of 21 immune checkpoints were decreased in high risk score group, while ULBP1 was increased in high risk score group in comparison with low risk score group.

3.7. The drug sensitivity of signatures in GDSC and CTRP databases

To explore the function of four signatures in chemotherapy, the expression of four signatures and drug sensitivity were integrated through GDSC and CTRP databases. According to CTRP database, we found MFAP2 was positively related to some drugs including GSK525762A, GW-405833 and I-BET151, while MATN4, LGI4 and FGL2 were negatively and significantly related to numerous drugs, such as AT13387, BIX-01294 and BMS-345541 (Fig. 8A). Meanwhile, the analysis of GDSC database demonstrated that LGI4 were significantly and negatively correlated to PD-0325901 and phenformin, which was respectively opposed to MATN4 and MFAP2 (Fig. 8B). Moreover, MFAP2 was positively related to most drug sensitivity in GDSC database, while MATN4 and FGL2 were negatively related to most drug sensitivity (Fig. 8B). Taken together, MFAP2 mainly played a positive role in drug sensitivity, while the effect of MATN4, LGI4 and FGL2 were negative on drug sensitivity.

4. Discussion

Previous studies identified that ECM played a crucial role in the growth and development of various tumors [21]. In our study, the expression profile and PCA analysis suggested that ECM-core genes to a great extent contributed to the progress of LSCC. Thus, on the basis of differentially expressed ECM-core genes in TCGA and GEO datasets, we constructed a 4-gene prognosis model with high stability and effectiveness. Moreover, four genes, namely MATN4, FGL2, MFAP2 and LGI4, and risk scores had an independent predicting value in the DSS time of LSCC.

Numerous genes played essential roles in the complex progress of cancer [22]. MATN4 is an adaptor protein of ECM, but the function of MATN4 was reported by few studies [23,24]. Uckelmann et al. identified that MATN4 was upregulated in hematopoietic stem cells (HSC) and silencing MATN4 resulted in promoting the proliferation of HSC after acute stress [25]. It indicated that MATN4 is a tumor suppressor in HSC. FGL2 is a transmembrane protein with 439 amino acids distributed in ECM and originated from T lymphocytes [26,27]. Some studies identified that FGL2 had a promoting function in the development of some cancers, including glioma stem cells and cutaneous squamous cell carcinoma [28,29]. In vitro experiments, silencing FGL2 could cause cell cycle arrest in

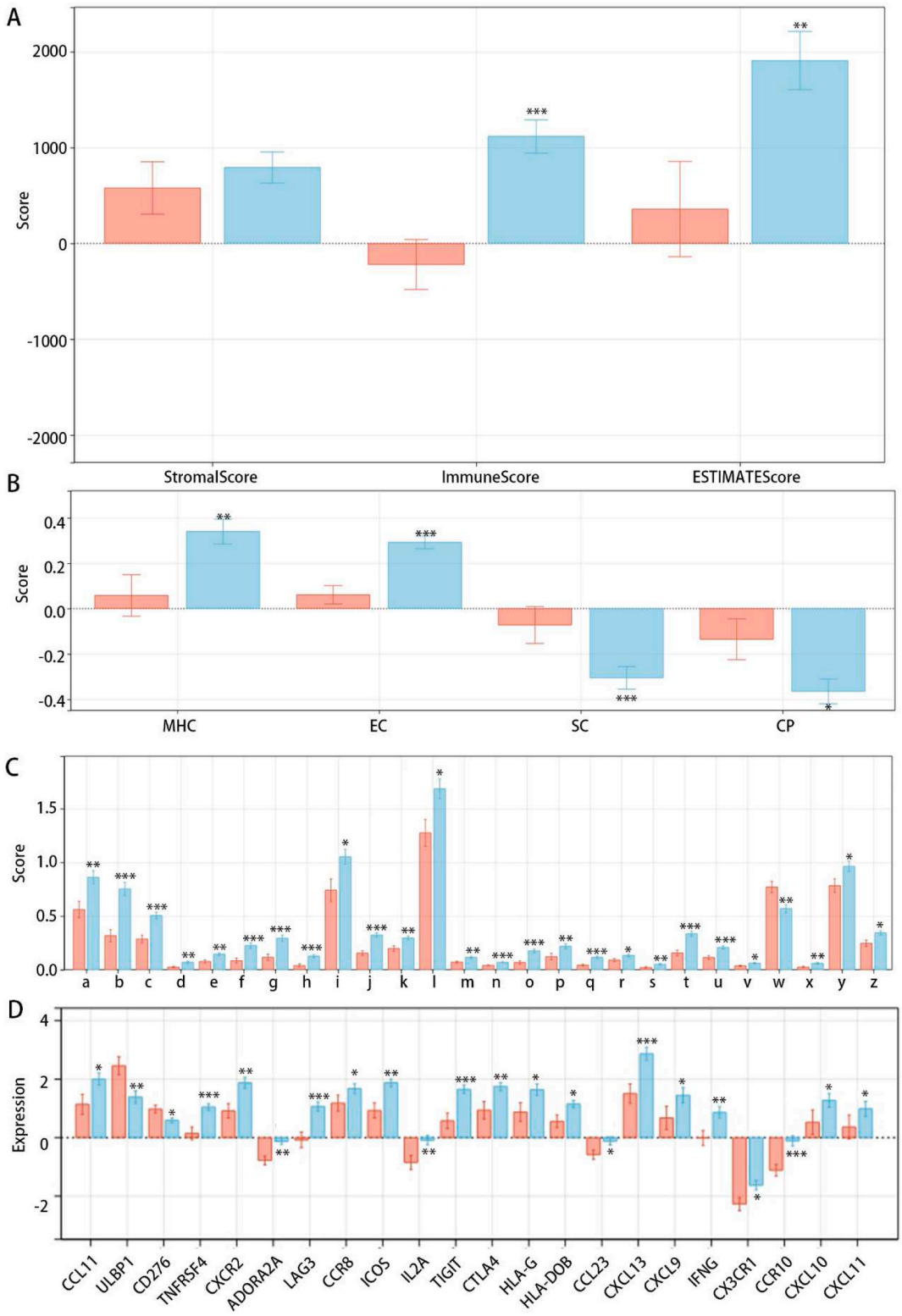

(caption on next page)

Fig. 7. The comparison with high and low risk score group in immune infiltration. The red group indicated high risk score; the blue group indicated low risk score. (A) ESTIMATE analysis, (B) IPS analysis, (C) The immune cell (D) The immune checkpoints expression in tumor and normal group. a: aDC, b: B-cells, c: $CD4^+$ memory T-cells, d: $CD4^+$ naïve T-cells, e: $CD4^+$ T-cells, f: $CD8^+$ T-cells, g: $CD8^+$ Tcm, h: $CD8^+$ Tem, i: cDC, j: class-switched memory B-cells, k: DC, l: iDC, m: mast cells, n: megakaryocytes, o: memory B-cells, p: monocytes, q: naïve B-cells, r: neutrophils, s: NK cells, t: pDC, u: plasma cells, v: platelets, w: smooth muscle, x: Tgd cells, y: Th1 cells, z: Tregs.

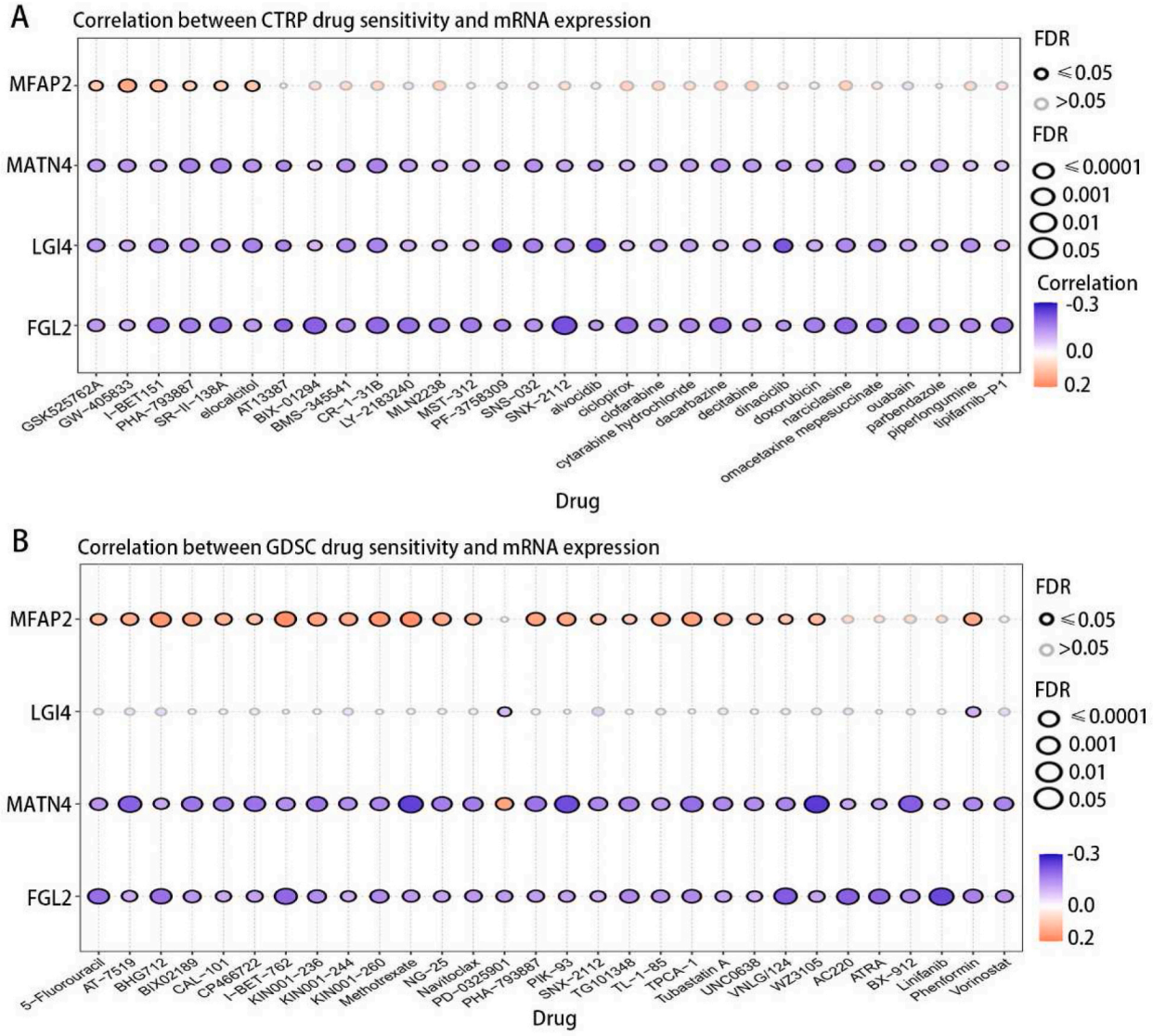

Fig. 8. The correlation of four signatures and multiple drugs based on (A) GDSC and (B) CTRP database.

hepatocellular carcinoma cells, which had a negative effect on the proliferation of tumor cells [30]. Costa et al. determined that upregulated LGI4 could promote the development of breast cancer cells [31]. Besides, Luo et al. found that LGI4 could be an independent predicting factor for the overall survival in colon cancer [32]. LGI4 is a member of the LGI family [33], and most researchers focus on the function of LGI4 in the nervous system [34,35].

Moreover, ECM was also involved in tumor development through affecting immune response and signal pathways [36]. MFAP2 is a member of MFAPs, which play a role in regulating the growth factor signal transduction [37]. Yao et al. identified that MFAP2 was involved in the regulation of cancer development through activating the ERK1/2 signal pathway in gastric cancer [38]. Additionally, Chen et al. found that MFAP2 regulated the metastasis of melanoma through mediating the WNT signal pathway [39], which plays a crucial role in immune response [40]. Besides, Zhu et al. claimed that the positive effect of MFAP2 on the development of hepatocellular carcinoma cells may depend on the interaction with immune factors [41]. Furthermore, FGL2 also performed a vital role in the immune response. Previous studies identified that FGL2 could induce immune response through polarizing macrophages and

promoting the proliferation of Treg cells and upregulating the expression of PD-1 [42,43]. Although the functions of MATN4 and LGI4 in tumor development were not clear at present, FGL2 and MFAP2 were closely related to the immune response. In this work, ssGSEA analysis revealed that the risk score had a high correlation with immune-related progress and signal pathways. Besides, GO and KEGG analysis revealed that genes related to four signatures were enriched in immune progress and some signal pathways which was involved in the immune progress. These results indicated that four signatures were closely related to the immune response. The further results showed that risk score was negatively and significantly related to most immune cells and immune checkpoints. It further suggested that signatures may inhibit the development of LSCC cells through activating immune cells. Similarly, Zhao et al. identified that the risk score constructed by 6 ECM-related genes was positively and closely related to immune cells, and the prediction model combined 6 hub genes with age, grade and stage had higher predictive efficiency in BLCA (35450397). Besides, Ahluwalia et al. constructed a risk model based on 12 ECM-related genes in clear cell renal clear cell carcinoma, and the high risk score group with ECM-rich had a high infiltration of T-regulatory and macrophages (33828127). It also indicated that ECM-related genes play a vital role through mediating immune response. In addition, they also demonstrated that the risk score was affected by age and TNM stage. In our study, we found that the risk score was only remarkably affected by N stage, which suggested that this risk model was more steadily for the clinical diagnose.

At present, ECM had been considered a key factor of drug resistance in tumor treatments [44,45]. Previous studies determined that ECM stiffness could affect drug sensitivity through various mechanisms [19]. On the one hand, ECM stuffiness could affect the sensitivity of tumor cells to numerous drugs through mediating signal pathways, such as c-Jun N-terminal kinase (JNK) and noncanonical nuclear factor-kappaB (NF-κB) signal pathways [46]. In this study, we identified that MFAP2 was positively related to the sensitivity of some drugs, while FGL2, LGI4 and MATN4 was negatively associated with the sensitivity of many drugs. It indicated that the better choice of drug in clinical treatment could be determined according to the correlation between expressions of signatures and drug sensitivity.

In conclusion, we constructed a four-genes risk model which showed a great prognosis value in the DSS of LSCC. Besides, we found these genes were closely related to the immune response through affecting the activation of immune cells and immune checkpoints. Furthermore, we identified the relationship between signatures and many drugs, which could improve the chemotherapy and targeted therapy for LSCC patients. Unfortunately, because of the lack of LSCC dataset with survival information, we could not validate the efficiency of risk model using independent datasets. But it is the first time that ECM-related risk model was used in the prognosis of LSCC, and our risk model was not affected by most clinical characteristics, which meant this model could be effectively and widely applied for most patients with LSCC. We believe that these results could provide a theoretical basis for further research and clinical treatment in the future.

Author contribution statement

Conception and design: Xue-fan Jiang. Collection and assembly of data: Wen-jing Jiang.

Data analysis and interpretation

All authors.

Data availability statement

Data will be made available on request.

Funding statement

Not applicable.

Consent for publication

Not applicable.

Ethical approval and consent to participate

The Ethics Committee of Zhejiang Provincial People's Hospital deemed that this research is based on open-source data, so the need for ethics approval was waived.

Declaration of competing interest

The authors declare that they have no known competing financial interests or personal relationships that could have appeared to influence the work reported in this paper.

Acknowledgement

Not applicable.

Appendix A. Supplementary data

Supplementary data to this article can be found online at https://doi.org/10.1016/j.heliyon.2023.e19907.

References

[1] X. Wang, et al., RBM15 facilitates laryngeal squamous cell carcinoma progression by regulating TMBIM6 stability through IGF2BP3 dependent, J. Exp. Clin. Cancer Res. 40 (1) (2021) 80.
[2] G. Zhou, et al., Comprehensive analysis reveals COPB2 and RYK associated with tumor stages of larynx squamous cell carcinoma, BMC Cancer 22 (1) (2022) 667.
[3] Y. Wu, et al., Circular RNA circCORO1C promotes laryngeal squamous cell carcinoma progression by modulating the let-7c-5p/PBX3 axis, Mol. Cancer 19 (1) (2020) 99.
[4] Z. Qian, et al., Heterogeneity analysis of the immune microenvironment in laryngeal carcinoma revealed potential prognostic biomarkers, Hum. Mol. Genet. 31 (9) (2022) 1487–1499.
[5] F. Dai, et al., MicroRNA-375 inhibits laryngeal squamous cell carcinoma progression via targeting CST1, Braz J Otorhinolaryngol 88 (Suppl 4) (2022) S108–S116. Suppl 4.
[6] L. Bruine de Bruin, et al., High DNMT1 is associated with worse local control in early-stage laryngeal squamous cell carcinoma, Laryngoscope 132 (4) (2022) 801–805.
[7] M. Cavaliere, et al., Biomarkers of laryngeal squamous cell carcinoma: a review, Ann. Diagn. Pathol. 54 (2021), 151787.
[8] J. Wang, et al., APE1 facilitates PD-L1-mediated progression of laryngeal and hypopharyngeal squamous cell carcinoma, Int. Immunopharm. 97 (2021), 107675.
[9] M. Najafi, B. Farhood, K. Mortezaee, Extracellular matrix (ECM) stiffness and degradation as cancer drivers, J. Cell. Biochem. 120 (3) (2019) 2782–2790.
[10] H. Chang, et al., Silencing gene-engineered injectable hydrogel microsphere for regulation of extracellular matrix metabolism balance, Small Methods 6 (4) (2022), e2101201.
[11] V. Mohan, A. Das, I. Sagi, Emerging roles of ECM remodeling processes in cancer, Semin. Cancer Biol. 62 (2020) 192–200.
[12] L. Beunk, et al., Cancer invasion into musculature: mechanics, molecules and implications, Semin. Cell Dev. Biol. 93 (2019) 36–45.
[13] B. Piersma, M.K. Hayward, V.M. Weaver, Fibrosis and cancer: a strained relationship, Biochim. Biophys. Acta Rev. Canc 1873 (2) (2020), 188356.
[14] F.L. Miles, R.A. Sikes, Insidious changes in stromal matrix fuel cancer progression, Mol. Cancer Res. 12 (3) (2014) 297–312.
[15] A.E. Yuzhalin, et al., Dynamic matrisome: ECM remodeling factors licensing cancer progression and metastasis, Biochim. Biophys. Acta Rev. Canc 1870 (2) (2018) 207–228.
[16] A.D. Theocharis, et al., Extracellular matrix structure, Adv. Drug Deliv. Rev. 97 (2016) 4–27.
[17] D.A.C. Walma, K.M. Yamada, The extracellular matrix in development, Development 147 (10) (2020).
[18] L. Yang, et al., Extracellular matrix and synapse formation, Biosci. Rep. 43 (1) (2023).
[19] Y. Jiang, et al., Targeting extracellular matrix stiffness and mechanotransducers to improve cancer therapy, J. Hematol. Oncol. 15 (1) (2022) 34.
[20] I. Eke, N. Cordes, Focal adhesion signaling and therapy resistance in cancer, Semin. Cancer Biol. 31 (2015) 65–75.
[21] H. Zhao, et al., Prediction of prognosis and recurrence of bladder cancer by ECM-related genes, J Immunol Res 2022 (2022), 1793005.
[22] R. Sahu, S.P. Pattanayak, Strategic developments & future perspective on gene therapy for breast cancer: role of mTOR and brk/PTK6 as molecular targets, Curr. Gene Ther. 20 (4) (2020) 237–258.
[23] P. Li, et al., Mice lacking the matrilin family of extracellular matrix proteins develop mild skeletal abnormalities and are susceptible to age-associated osteoarthritis, Int. J. Mol. Sci. 21 (2) (2020).
[24] S. Zhang, et al., Matrilin-2 is a widely distributed extracellular matrix protein and a potential biomarker in the early stage of osteoarthritis in articular cartilage, BioMed Res. Int. 2014 (2014), 986127.
[25] H. Uckelmann, et al., Extracellular matrix protein Matrilin-4 regulates stress-induced HSC proliferation via CXCR4, J. Exp. Med. 213 (10) (2016) 1961–1971.
[26] S. Marazzi, et al., Characterization of human fibroleukin, a fibrinogen-like protein secreted by T lymphocytes, J. Immunol. 161 (1) (1998) 138–147.
[27] J. Yu, et al., The role of Fibrinogen-like proteins in Cancer, Int. J. Biol. Sci. 17 (4) (2021) 1079–1087.
[28] J. Yan, et al., FGL2 promotes tumor progression in the CNS by suppressing CD103(+) dendritic cell differentiation, Nat. Commun. 10 (1) (2019) 448.
[29] M. Zeng, et al., The Fgl2 interaction with Tyrobp promotes the proliferation of cutaneous squamous cell carcinoma by regulating ERK-dependent autophagy, Int. J. Med. Sci. 19 (1) (2022) 195–204.
[30] M. Wang, et al., Adenovirus-mediated artificial microRNA against human fibrinogen like protein 2 inhibits hepatocellular carcinoma growth, J. Gene Med. 18 (7) (2016) 102–111.
[31] E.T. Costa, et al., Intratumoral heterogeneity of ADAM23 promotes tumor growth and metastasis through LGI4 and nitric oxide signals, Oncogene 34 (10) (2015) 1270–1279.
[32] Y. Luo, et al., Integrated bioinformatics analysis to identify abnormal methylated differentially expressed genes for predicting prognosis of human colon cancer, Int. J. Gen. Med. 14 (2021) 4745–4756.
[33] V. Herranz-Perez, et al., Regional distribution of the leucine-rich glioma inactivated (LGI) gene family transcripts in the adult mouse brain, Brain Res. 1307 (2010) 177–194.
[34] J. Nishino, et al., Lgi4 promotes the proliferation and differentiation of glial lineage cells throughout the developing peripheral nervous system, J. Neurosci. 30 (45) (2010) 15228–15240.
[35] E. Ozkaynak, et al., Adam22 is a major neuronal receptor for Lgi4-mediated Schwann cell signaling, J. Neurosci. 30 (10) (2010) 3857–3864.
[36] C.E. McQuitty, et al., Immunomodulatory role of the extracellular matrix within the liver disease microenvironment, Front. Immunol. 11 (2020), 574276.
[37] C.S. Craft, T.J. Broekelmann, R.P. Mecham, Microfibril-associated glycoproteins MAGP-1 and MAGP-2 in disease, Matrix Biol. 71–72 (2018) 100–111.
[38] L.W. Yao, et al., MFAP2 is overexpressed in gastric cancer and promotes motility via the MFAP2/integrin alpha5beta1/FAK/ERK pathway, Oncogenesis 9 (2) (2020) 17.
[39] Z. Chen, et al., Microfibril-associated protein 2 (MFAP2) potentiates invasion and migration of melanoma by EMT and wnt/beta-catenin pathway, Med. Sci. Mon. Int. Med. J. Exp. Clin. Res. 26 (2020), e923808.
[40] Y. Zhou, et al., Wnt signaling pathway in cancer immunotherapy, Cancer Lett. 525 (2022) 84–96.
[41] X. Zhu, et al., MFAP2 promotes the proliferation of cancer cells and is associated with a poor prognosis in hepatocellular carcinoma, Technol. Cancer Res. Treat. 19 (2020), 1533033820977524.
[42] K. Latha, et al., The role of fibrinogen-like protein 2 on immunosuppression and malignant progression in glioma, J. Natl. Cancer Inst. 111 (3) (2019) 292–300.
[43] J. Yan, et al., FGL2 as a multimodality regulator of tumor-mediated immune suppression and therapeutic target in gliomas, J. Natl. Cancer Inst. 107 (8) (2015).

[44] A. Hosseini, et al., Role of the bone marrow microenvironment in drug resistance of hematological malignances, Curr. Med. Chem. 29 (13) (2022) 2290–2305.
[45] H. Ji, et al., Identification of stromal microenvironment characteristics and key molecular mining in pancreatic cancer, Discov Oncol 13 (1) (2022) 83.
[46] A.P. Drain, et al., Matrix compliance permits NF-kappaB activation to drive therapy resistance in breast cancer, J. Exp. Med. 218 (5) (2021).